Traffic & Transportation

A Fuzzy Neural Network-Based Robust Control Algorithm for the Trajectory of a Roadway Inspection Robot

Yali YANG[1], Xuelei ZHAO[2], Zhibo YANG[3]

Original Scientific Paper
Submitted: 18 Feb 2025
Accepted: 21 May 2025
Published: 30 Mar 2026

[1] Corresponding author, yangyali2024@163.com, Department of Basic Education, Shangqiu Institute of Technology, Shangqiu, China
[2] zhaoxuelei2024@163.com, Department of Basic Education, Shangqiu Institute of Technology, Shangqiu, China
[3] yangzhibo202412@163.com, Department of Basic Education, Shangqiu Institute of Technology, Shangqiu, China

Publisher:
Faculty of Transport and Traffic Sciences, University of Zagreb

ABSTRACT
In order to meet the requirements of complex tunnel inspection and ensure the reliable operation of inspection robots under external interference and terrain changes, a trajectory robust control algorithm based on a fuzzy neural network is proposed. This algorithm combines the motion characteristics of the inspection robot to analyse the motion variables that affect the trajectory. The deviation and deviation rate of the left and right track running speed and steering angle are used as control variables and input into the PID controller. By adjusting PID parameters online through fuzzy neural networks, a PID robust controller is constructed to achieve trajectory control. Tests have shown that the controller performs best when the PID control parameters are set to 0.25, 0.65 and 0.55. The steering angle robustness margin is less than 2° in both single and complex scenarios, and the maximum trajectory deviation is only (0.3,0) cm, effectively achieving robust trajectory control of the tunnel inspection robot.

KEYWORDS
fuzzy neural network; roadway inspection; robot; trajectory robust control; motion variables; control variables.

1. INTRODUCTION

Roadway inspection robot is a kind of intelligent robot designed specifically for the roadway environment [1]. It is widely used in subways, mines, tunnels and other underground or closed spaces that require inspection. The robot regularly inspects and monitors the equipment and structures inside the roadway [2]. It monitors and records environmental parameters in real time, such as temperature, humidity and gas concentration (gas, carbon monoxide, etc.). Simultaneously, the robot detects the operation of equipment in the tunnel. When it detects issues such as equipment failure, structural deformation or safety hazards, the robot immediately issues an alarm and records the abnormalities [3]. This helps management personnel take timely measures to ensure the normal operation of the inspected areas. In the roadway inspection task, the robot needs to face the complex and changing environment, such as obstacles, light changes, ground inequality, etc. These factors may lead to the robot's trajectory tracking performance degradation [4] and even lead to its disorientation or collision.

Therefore, it is important to study a robust trajectory control algorithm to improve the inspection efficiency and safety of the robot [5]. Through the accurate trajectory control, the roadway inspection robot can be in accordance with the predetermined path to carry out efficient [6] and accurate inspection. To ensure the reliability of the robot's movement trajectory, a camera mounted on the robot's end-effector is used to determine the optimal distance between the sensor and the surface to be scanned. Once this distance is established, the robot autonomously generates a scanning trajectory over the unknown surface. For surfaces with a known shape but unknown location, the robot first determines the position of the surface before initiating

the scan to ensure reliable trajectory generation. When applying the proposed method to unknown surfaces with complex or highly irregular shapes, image quality may be affected by several factors, such as lighting conditions and the surface material. These factors can result in unclear or distorted images captured by the camera, which in turn can compromise the reliability of the movement trajectory [7]. Morlock et al. applied the concept of servo constraints to generate an inverse model of the robot for robot trajectory control, analysed the motion characteristics of the robot during the motion process and combined the analysis results with the known linear quadratic regulator (LQR) for trajectory tracking based on differential and algebraic equations. Algebraic equations for trajectory tracking, combined with the servo constraints of the input-output feedback linearisation method, are used to control a flexible link parallel robot by tracking a redefined trajectory. However, flexible link robots are typically more sensitive to external disturbances (e.g., vibrations, load changes). During practical application, the control method shows relatively poor disturbance rejection capability, which can lead to increased trajectory tracking errors [8]. Baji et al. proposed a trajectory tracking control method for SCARA robots based on inverse dynamics using both numerical and symbolic computation. This method analyses the explicit form of the robot's equations of motion to represent the relationship between joint positions, velocities, accelerations and driving forces. By leveraging this explicit form, the system achieves real-time online trajectory tracking control during the operation. During the control process, the system obtains the current state of the robot in real time and calculates the required driving force according to the preset trajectory planning, and realises the trajectory tracking by inputting the calculated driving force into the robot to make it move along the preset trajectory. During the application process of the method, the system combining inverse dynamics numerical and symbolic computation may show low robustness in the face of the external disturbances or uncertainty of the model. This may lead to trajectory tracking errors or instability of SCARA robots in actual operation [9]. Salvioli et al. used dynamic programming algorithms to decompose the complex whole-body motion planning problem into a series of sub problems, and used the optimal solution of each sub problem to solve the optimal solution of the overall problem. Dynamic programming can consider factors such as robot motion constraints and environmental obstacles to obtain the best trajectory results. Dynamic planning can take into account the robot's motion constraints, environmental obstacles and other factors, so as to obtain the best trajectory results. Although the dynamic planning algorithm selects the best decision at each stage to ensure global optimality, it can become time-consuming in complex environments. This increased computation time reduces real-time control performance. Furthermore, if there are discrepancies between the model and the actual robot, the planning results may be inaccurate or even infeasible to execute [10].

Fuzzy neural networks combine the advantages of fuzzy logic and neural networks, making them a widely studied intelligent control method in recent years. Fuzzy logic handles uncertainty and ambiguity in systems, while neural networks offer strong learning and adaptability. By integrating these two approaches [11], fuzzy neural networks effectively control complex systems. Therefore, in this paper, in order to realise the trajectory control of the roadway inspection robot, the fuzzy neural network is taken as the core and combined with the PID controller to carry out robust control. The fuzzy neural network can deal with the uncertainty and nonlinear factors in the roadway environment, such as changes in the terrain, the distribution of obstacles and so on. Moreover, the fuzzy neural network can adaptively adjust the PID control parameters to realise the precise control of the robot trajectory, which can resist the external interference and internal changes to a certain extent and ensure the stable operation of the robot.

2. IMPLEMENTATION OF ROBUST CONTROL OF THE TRAJECTORY OF AN ALLEY INSPECTION ROBOT

In order to realise the effective robust control of the trajectory of the roadway inspection robot, the motion characteristic analysis of the roadway inspection robot is carried out to clarify the key control variables and lay the foundation for the subsequent control.

2.1 Motion characterisation of alleyway inspection robot

When the roadway inspection robot is running, the left and right side tracks are parallel and in the same direction [12], and the centre of mass O of the inspection robot coincides with the geometric centre of its body. Therefore, in order to ensure the robust control effect of the robot trajectory, the motion model of the roadway inspection robot is constructed in this paper to analyse the kinematics of the coal mine inspection robot [13]. The motion state of the roadway robot is shown in *Figure 1*.

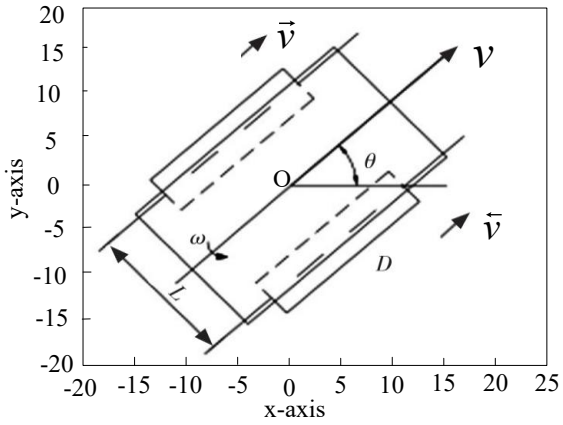

Figure 1 – Motion state of tunnel robot

Since the size of the sliding coefficient of the track of the coal mine inspection robot in the coal mine tunnel depends on factors such as the track and the condition of the tunnel floor [14], assuming that the coal mine inspection robot operates under ideal conditions and does not slip, the current position vector $q=[x,y,\vartheta]^T$ of the robot mass point P, according to the kinematics principle of the inspection robot, the operation formula of the inspection robot is:

$$\begin{cases} v=\dfrac{\vec{v}+\bar{v}}{2} \\ \vec{v}=\dfrac{\vec{\omega}D}{2} \\ \bar{v}=\dfrac{\bar{\omega}D}{2} \end{cases} \tag{1}$$

$$\omega=\dot{\vartheta}=\frac{\vec{v}-\bar{v}}{L} \tag{2}$$

where: v, $\vec{v}$, $\bar{v}$ indicate the running speed of the body and the left and right tracks. ω, $\vec{\omega}$, $\bar{\omega}$ denote the angular velocity of rotation of the body and the left and right tracks, respectively. ϑ denotes the relative steering angle of the roadway robot patrol; $\dot{\vartheta}$ denotes the first order derivative of the relative steering angle; L indicates the distance between left and right track centres. D indicates the diameter of the track drive wheel.

If the coal mine inspection robot operates under the ideal condition of no sliding, its inspection robot is subject to non-integrity constraints, combined with the simplified processing of *Equation (1)*, the kinematic model of its inspection robot can be obtained as follows:

$$\dot{q}=\begin{bmatrix}\dot{x}\\ \dot{y}\\ \dot{\vartheta}\end{bmatrix}=\begin{bmatrix}v\\ \omega\end{bmatrix}\begin{bmatrix}\cos\vartheta & -\dfrac{D}{2}\sin\vartheta\\ \sin\vartheta & \dfrac{D}{2}\cos\vartheta\\ 0 & 1\end{bmatrix} \tag{3}$$

where: $\dot{x}$ and $\dot{y}$ denote the first order derivative of the axis offset for X axis and Y axis; $\dot{q}$ denotes the first-order derivative of the current position vector.

The following can be observed from *Equation (3)*: during the movement of the coal mine inspection robot in the roadway, by controlling the left and right track speed $\vec{v}$, $\bar{v}$ and the steering angle ϑ of the inspection robot, the trajectory control can be realised.

2.2 Robust control of trajectory based on fuzzy neural network with PID controller

PID control structure with fuzzy neural networks

Combined with the above subsections, it can be seen that, in order to ensure the robust trajectory control of roadway inspection robot, it is necessary to control the left and right track speed $\vec{v}$, $\bar{v}$ and steering angle ϑ . A PID control system based on a fuzzy neural network is constructed for this purpose. The overall system consists of two parts: a PID robust controller and a fuzzy neural network. The structure of the fuzzy neural network-based PID controller is shown in *Figure 2*.

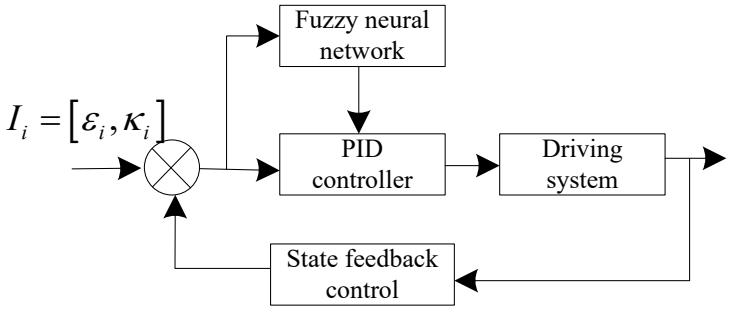

Figure 2 – Robust controller structure based on fuzzy neural network PID

In the controller, the PID robust controller is mainly used to realise the closed loop control of the left and right track running speed $\vec{v}$ and $\bar{v}$ and the steering angle ϑ of the roadway inspection robot. The fuzzy neural network is mainly used to realise the online adjustment of the control parameters of the PID controller so as to improve the control effect of the robot trajectory [15]. The fuzzy neural network PID robust control formed in this way has the stability of traditional PID control, the reasoning ability of fuzzy control and the learning ability of neural network, which can complete the stable and fast adjustment under different inspection conditions and environments to ensure the control effect of the trajectory of the roadway inspection robot [16].

Fuzzy neural network-based PID control parameter correction

In order to ensure the trajectory control effect of the roadway inspection robot, based on the above structure, a fuzzy neural network is utilised to carry out the online adjustment of PID control parameters. The adjustment of PID control parameters is completed according to the deviation of the left and right track speed $\vec{v}$, $\bar{v}$, its steering angle ϑ and its deviation rate. Through the adjustment, the trajectory control amount of the roadway inspection robot is obtained, and the control amount is the speed error and steering angle error of the robot. Considering that the trajectory error and attitude error control principle is the same [17], REF neural network and fuzzy control theory are combined to form a fuzzy neural network. This network combines REF neural network optimisation learning to extract features and patterns from a large amount of nonlinear data, accurately describing and predicting the motion state of the robot [18]. At the same time, fully combining fuzzy control theory, it can handle uncertainty and fuzzy data in the system, and solve the problem of insensitivity to small changes in input data. It can adaptively adjust according to actual situations, ensure good robustness, and enable the robot to operate stably in various complex environments.

Parameter adjustment is the core step in robust trajectory control of tunnel inspection robots based on fuzzy neural networks. Fuzzy neural networks, through their built-in learning algorithms, utilise the mapping relationship between input and output data to continuously adjust the connection weights and biases within the network, aiming to minimise prediction errors. This process is specifically reflected in the online dynamic correction of three key control parameters in the PID controller: proportional (Kp), integral (Ki) and derivative (Kd). The adjustment of PID parameters is directly related to the dynamic response characteristics of the system: Kp determines the response speed of the system, Ki is used to eliminate steady-state errors and Kd helps improve the dynamic performance of the system, reduce overshoot and oscillation. Fuzzy neural networks, with their powerful learning and adaptive capabilities, can perceive the real-time operating status of robots (such as speed error, steering angle error and their rate of change), and dynamically adjust PID parameters accordingly to achieve optimal control effects. In the control process of the tunnel inspection robot,

the dynamic adjustment of PID parameters can help the system balance speed, accuracy and stability. For example, when the robot encounters a large obstacle causing an increase in speed error, the fuzzy neural network can timely increase Kp to accelerate the response, while adjusting Ki to eliminate the accumulation of speed deviation. By adjusting Kd, speed fluctuations and oscillations can be reduced, ensuring that the robot can operate stably in complex and changing tunnel environments.

The fuzzy neural network has six layers: input layer, fuzzification layer, fuzzy inference layer, normalisation layer, fuzzy solution layer and output layer, and its overall structure is shown in *Figure 3*.

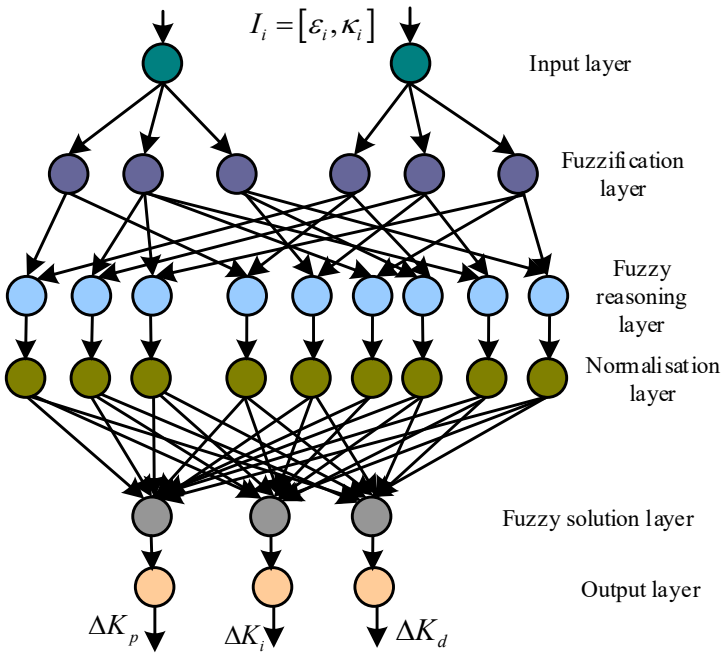

Figure 3 – Fuzzy neural network structure

The first layer is the input layer. The role of this layer is to transmit the input data corresponding directly to the second fuzzification layer. The number of neurons in this layer is $N_1 = 6$, i.e. six input variables, namely, which are deviation $\Delta\vec{v}$ and deviation change rate $\vec{\kappa}$ of left track running speed of roadway inspection robot $\vec{v}$, deviation $\Delta\bar{v}$ and deviation change rate $\bar{\kappa}$ of left crawler running speed $\bar{v}$, deviation $\Delta\theta$ of steering angle ϑ and its deviation rate κ_θ respectively, forming the 6 variables into input variables, using $I_i = [\varepsilon_i, \kappa_i]$ to denote, where ε_i contains $\Delta\vec{v}$, $\Delta\bar{v}$ and $\Delta\theta$, κ_i contains $\vec{\kappa}$, $\bar{\kappa}$ and κ_θ. Then the input layer is given by:

$$O_i^1 = I_i^1 \tag{5}$$

where: O_i^1 indicates the output of the first layer.

The second layer is the fuzzification layer. The parameters of the nodes in this layer are the fuzzy variables and their affiliation results. Taking the above output O_i^1 as the input of this layer, it corresponds to two fuzzy linguistic variables, that is to say, in the first layer, the first five neurons of the speed of motion are taken as the input parameters, which correspond to two fuzzy linguistic neurons of the defuzzification layer. The input steering angle parameter corresponds to five fuzzy linguistic variables, that is to say, the sixth neuron of the first layer is taken as the input steering angle parameter, which corresponds to five fuzzy linguistic neurons of the defuzzification layer. To calculate the affiliation function of each node in the layer, the Gaussian function is chosen as the affiliation function in the paper, and the output of the layer is calculated as follows:

$$O_{ij}^2 = \exp\left[-\frac{O_i^1 - c_{ij}}{\varsigma_{ij}^2}\right]^2 \tag{6}$$

where: c_{ij} and ς_{ij}^2 denote the j th membership function centre and width of the i th variable.

The third layer is the fuzzy rule layer. This layer corresponds to the fuzzy inference process of the whole fuzzy neural network [19], in which the matching degree of the corresponding fuzzy variables is calculated mainly by obtaining the affiliation degree of different fuzzy neurons, in which each fuzzy rule corresponds to a node, and the specific affiliation degree calculation formula is as follows:

$$O_l^3 = O_{ij}^2 \xi_1 \xi_2 \xi_3 \xi_4 \xi_5 \xi_6 \tag{7}$$

where: ξ_1, ξ_2, ξ_3, ξ_4, ξ_5, ξ_6 denote the affiliation function of the variables $\Delta\vec{v}$, $\vec{\kappa}$, $\vec{\kappa}$, $\Delta\vec{v}$, $\Delta\theta$, κ_θ.

When determining fuzzy rules in this layer, the variable domain theory is introduced to design a scaling factor, which ensures the completeness of the fuzzy rules and makes their rule settings reasonable [20], avoiding affecting control performance and meeting the trajectory control requirements of the tunnel inspection robot, in order to respond to its dynamic changes and environmental changes in a timely manner. This process combines the characteristics of input variable $I_i = [\varepsilon_i, \kappa_i]$ and uses a function model to set scaling factors separately. The design formula is:

$$\alpha(\varepsilon_i) = \left[\frac{|\varepsilon_i(t)|}{G_1}\right]^{\eta_1} + \chi \tag{8}$$

$$\alpha(\kappa_i) = \left[\frac{|\kappa_i(t)|}{G_2}\right]^{\eta_2} + \chi \tag{9}$$

$$\beta(I_i) = \frac{\left[\frac{|\varepsilon_i(t)|}{G_1}\right]^{\eta_3} + \left[\frac{|\kappa_i(t)|}{G_2}\right]^{\eta_4}}{2} \tag{10}$$

where: α and β denote the scaling factor. The initial thesis domain of ε_i is $[-G_1, G_1]$, the initial thesis domain of κ_i is $[-G_2, G_2]$; η_1, η_2, η_3, η_4 are parameters denoting the scaling factor; χ denotes the factor constants.

However, the expansion factor has no specific physical meaning and it needs to be set to a fixed value in practical application, which also makes the expansion factor not adaptive [21]. In this paper, in order to address this problem, considering the comparison of multiple experimental results and the principle of expansion factor selection, the factor design parameters are adjusted according to the error ε_i and error change rate κ_i. The calculation formula is as follows:

$$\eta_1 = \frac{1}{|\varepsilon_i(t)|(E_1 + E_2) + u} + \frac{1}{|\kappa_i(t)|(E_1 + E_2) + u} \tag{11}$$

where: u denotes a sufficiently small positive number.

To ensure the coordination of the input and output variables, take $\eta_1 = \eta_2 = \eta_3 = \eta_4$, and substituting into public positions (8), (9) and (10) yields a new functional type of expansion factor:

$$\alpha(\varepsilon_i) = \left[\frac{|\varepsilon_i(t)|}{E_1}\right]^{\eta_1} + \chi \tag{12}$$

$$\alpha\left(\kappa_i\right)=\left[\frac{\left|\kappa_i\left(t\right)\right|}{E_2}\right]^{\eta_2}+\chi \tag{13}$$

$$\beta\left(I_i\right)=\frac{\alpha\left(\varepsilon_i\right)+\alpha\left(\kappa_i\right)}{2}+\chi \tag{14}$$

The new functional expansion factor satisfies the requirements of monotonicity, parity, zero convergence, coordination and regularity in the selection of expansion factors, and is stable and effective [22]. Fuzzy neural network based on this new type of expansion factor can quickly adjust the deviation $\Delta\vec{v}$ of roadway inspection robot left track running speed $\vec{v}$ and deviation change rate $\vec{\kappa}$, deviation $\Delta\bar{v}$ of left track running speed $\bar{v}$ and deviation rate $\bar{\kappa}$, deviation $\Delta\theta$ of the steering angle ϑ and its deviation rate κ_θ. To obtain the corresponding membership function into the above formula (7), new membership results are obtained.

The fourth layer is the normalisation layer. To prepare for the clarity of the fuzzy results, the adaptation is scaled according to a certain percentage and the normalisation formula is:

$$\bar{O}_l^4=\frac{O_l^3}{\sum_{i=1}^{N_3}O_i^3} \tag{15}$$

where: N_3 denotes the number of neurons.

The fifth layer is the defuzzification layer. It is mainly used to realise the calculation of defuzzification and its calculation formula is as follows:

$$O_l^5=\sum_{i=1}^{N_4}w_l\bar{O}_l^4 \tag{16}$$

where: w_l denotes the weight, which represents the centre value of the affiliation degree corresponding to the obtained inference result. N_4 denotes the number of neurons.

The sixth layer is the output layer. This layer is used to output the mapping result of the domain, which is calculated as follows:

$$O_l^6=\hat{\Upsilon}O_l^5 \tag{17}$$

$$\begin{cases}\Delta K_p=O_1^6\\ \Delta K_i=O_2^6\\ \Delta K_d=O_3^6\end{cases} \tag{18}$$

where ΔK_p, ΔK_i and ΔK_d are the correction amounts of the three control parameters of the PID controller. In summary, based on the result of the correction amount of *Equation(18)*, the correction of PID control parameters is accomplished. Taking parameter K_d for example, the corrected results are shown in *Figure 4* below.

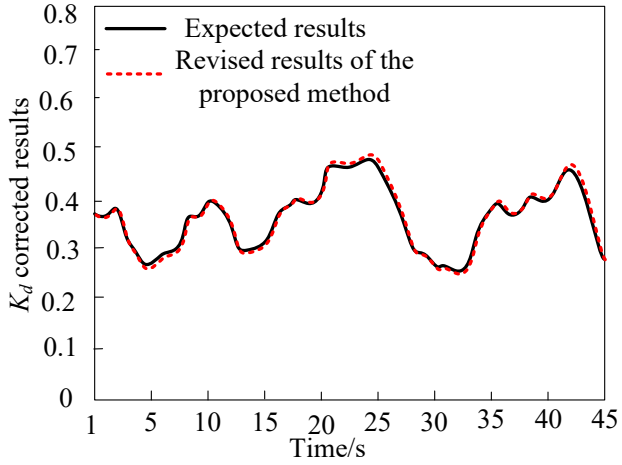

Figure 4 – PID control K_d parameter corrected results

The core of designing the scaling factor is to dynamically adjust the domain range of fuzzy rules based on the real-time state of the system, aiming to improve the adaptability and robustness of the controller. In this paper, the adjustment of the scaling factor is closely dependent on the error and its rate of change, which directly map the current control effect and dynamic evolution trend of the system. Specifically, when the error is significant, increasing the scaling factor can effectively broaden the domain of fuzzy rules, making the controller more sensitive to system state changes and accelerating response. On the contrary, when the error is small, reducing the scaling factor can refine the domain range and improve the resolution and stability of the controller. The calculation formula for the scaling factor contains multiple parameters selected based on in-depth analysis of the system's dynamic characteristics and extensive experimental verification. Its flexible adjustment ensures that the scaling factor can accurately adapt to control requirements in different environments. Especially in complex and ever-changing tunnel environments, facing diverse terrains, obstacles and interference factors, the real-time adjustment mechanism of the scaling factor enables the controller to maintain excellent control performance under various working conditions. In addition, this paper proposes a novel functional scaling factor that achieves adaptive adjustment of the scaling factor by incorporating real-time information on errors and error change rates, while meeting a series of strict selection principles.

Real-time control of trajectories based on a PID robust controller

For the online real-time correction of PID control parameters according to the control parameter correction amount ΔK_p, ΔK_i and ΔK_d output in the above section, the output formula of the controller is:

$$s(t)=\left(K_p+\Delta K_p\right)\varepsilon_i(t)+\left(K_i+\Delta K_i\right)\int_0^t \kappa_i(t)dt+ \left(K_d+\Delta K_d\right)\frac{d\varepsilon_i(t)}{dt} \tag{19}$$

Based on the results of *Equation (19)*, the robust control of the trajectory of the roadway inspection robot is performed to correct the deviation of the robot's trajectory and effectively inhibit the interference, so as to make the traveling belt inspection robot more robust to external perturbations and ensure the trajectory control accuracy.

The robust trajectory control of roadway inspection robot consists of PID control $s(t)$ and state feedback control $s_1(t)$. The specific control is:

$$\begin{cases} s_1(t)=f\left(\psi_1+\psi_2(t)\right)I_i \\ s(t)=\Delta(t-1)+\tilde{K}_p\left[\Delta(t)-\Delta(t-1)\right]+ \\ \quad \tilde{K}_i\Delta(t)+\tilde{K}_d\Delta(t)I_i \end{cases} \tag{20}$$

where ψ_1, $\psi_2(t)$ denote the fixed gain and auxiliary control matrix of the lane inspection robot; $f(.)$ denotes the prior distribution function; I_i indicates the control objective. $\tilde{K}_p$, $\tilde{K}_i$ and $\tilde{K}_d$ indicate the proportional, integral and differential control parameters of the modified PID.

Combining the computational results of *Equation (20)* to generate the robust control commands $\hat{S}$ for the trajectory of the alley inspection robot for the PID robust controller, which is calculated as follows:

$$\hat{S} = s_1(t)\mu_1 + s(t)\mu_2 - \varepsilon_i(t) - \kappa_i(t) \tag{21}$$

where μ_1 and μ_2 denote the control law and control parameters for PID control and state feedback control, respectively; $\varepsilon_i(t)$ and $\kappa_i(t)$, which are the velocity error and steering angle error of the robot.

According to the real-time update of the trajectory control quantity, the trajectory control command acting on the roadway inspection robot is derived, and the robust control of the roadway inspection robot trajectory is accomplished according to the control command.

3. TEST ANALYSIS

3.1 Test preparation

In order to verify the application effect of the control algorithm in the robust control of the trajectory of the roadway inspection robot, the roadway inspection robot used in a coal mine is used as an example to carry out the relevant tests, which is mainly used to replace the manpower to enter into the high-temperature, high-pressure, poisonous gases and other hazardous environments to carry out inspections, real-time monitoring of the roadway conditions, including the operating status of equipment, roadway deformation, ambient gas concentration, etc. and timely detection of potential safety hazards, such as gas leakage, fire, equipment failure, etc. The relevant parameters of the robot are shown in *Table 1*, and the site map of the inspection and testing environment is shown in *Figure 5*.

Table 1 – Parameters of tunnel inspection robot

Parameter	Numerical value
Maximum speed	1.5 m/s (stepless speed regulation)
Gradeability	≥ 40°(slope)
Stair climbing ability	≥ 34° (slope)
Height of obstacle crossing on flat ground	≥ 200 mm
Crossing ditch width	≥ 200 mm
Passage width	≥ 650 mm
Rotation function	Capable of rotating in place
Rotation angle	Continuous rotation with pitch ≥ 0°~90°and horizontal ≥ 0°~360°
Surveillance camera	≥ 30 x optical zoom, minimum illumination of 0.1 Lux
Intelligent functions	It can achieve autonomous obstacle avoidance, autonomous navigation, autonomous alarm and audio and video feedback
Ground clearance	≥ 100 mm
Remote control distance	Wireless ≥ 1000 m

Figure 5 – On site inspection and testing environment of the robot

When the algorithm in the paper is used to control the trajectory of the roadway inspection robot, it is necessary to make online real-time corrections to the three control parameters of the PID control to improve the control effect on the trajectory. Therefore, the results of the optimised control parameters $\tilde{K}_p$, $\tilde{K}_i$ and $\tilde{K}_d$ should be determined before testing the application effect of the algorithm. In this paper, the error result of linear trajectory and curve trajectory is used as indicators, and the parameters corresponding to the minimum result of the two indexes are the best values of $\tilde{K}_p$, $\tilde{K}_i$ and $\tilde{K}_d$ values. The test results are shown in *Table 2*.

Table 2 – Determination results of optimal control parameters

Take a value	Straight path /cm			Curve trajectory /cm		
	Proportion	**Integration**	**Differential**	**Proportion**	**Integration**	**Differential**
0.05	-0.48	0.42	0.31	0.39	0.33	0.29
0.15	0.52	-0.46	0.36	0.41	-0.35	-0.31
0.25	0.55	-0.49	-0.38	0.33	0.39	-0.35
0.35	-0.45	0.52	0.29	-0.34	-0.41	0.39
0.45	0.47	0.51	-0.36	-0.47	0.35	0.28
0.55	0.61	0.48	-0.41	0.45	0.37	-0.41
0.65	-0.53	-0.39	-0.39	0.54	-0.26	-0.35
0.75	0.51	-0.44	0.44	-0.46	-0.28	0.38
0.85	0.49	0.46	0.49	-0.51	-0.31	0.37
0.95	-0.55	0.53	-0.52	0.48	0.29	-0.43

By analysing the test results in *Table 2*, it can be seen that the algorithm in the text is based on different values of the $\tilde{K}_p$, $\tilde{K}_i$ and $\tilde{K}_d$ parameters for the trajectory control of the roadway inspection robot. Under different values of the parameters, the linear trajectory and curved trajectory error results show obvious differences in changes, where, under the linear inspection trajectory, the error is minimised when the $\tilde{K}_p$, $\tilde{K}_i$

and $\tilde{K}_d$ take the values of 0.25, 0.65 and 0.55 respectively, and under the curved inspection trajectory, the error is minimised when the $\tilde{K}_p$, $\tilde{K}_i$ and $\tilde{K}_d$ take the values of 0.35, 0.65 and 0.55 respectively. Comparing the test results under both trajectories, when $\tilde{K}_p$ takes the values of 0.25 and 0.35, the error values under the linear trajectory are 0.55 cm and -0.45 cm, respectively. The error values under the curved trajectory are 0.33 cm and -0.34 cm, respectively, i.e. under the linear trajectory, the difference between the error results of the two values is obvious, and that under the curved trajectory is smaller. Therefore, the parameters $\tilde{K}_p$, $\tilde{K}_i$ and $\tilde{K}_d$ take the value of 0.25, 0.65 and 0.55 and are used in the subsequent tests.

3.2 Test indicators

In order to verify the robustness of the algorithm in the trajectory control of the roadway inspection robot in the paper, the robustness margin is used as an evaluation index, which is used to describe the range of uncertainty that can be tolerated under the requirement of meeting certain performance indexes, and its value ranges from 0 to 2°. A larger robustness margin usually implies that the system has stronger robustness, and the total steering angle errors $\Delta\hat{\theta}_\Sigma$ under different working conditions are used in the paper as an indicator of this margin. The smaller its value is, the higher the robustness margin is. The formula for $\Delta\hat{\theta}_\Sigma$ is:

$$\Delta\hat{\theta}_\Sigma = \left|\sum_{t=1}^{T}\Delta\theta_1(t) - \sum_{t=1}^{T}\Delta\theta_2(t)\right| + \left|\sum_{t=1}^{T}\Delta\theta_1(t) - \sum_{t=1}^{T}\Delta\theta_3(t)\right| \tag{22}$$

where: $\Delta\theta_1(t)$, $\Delta\theta_2(t)$, $\Delta\theta_3(t)$ are the results of the steering angle errors of the alleyway robot during the inspection process without interference, indirect interference and continuous interference, respectively. T denotes the duration of the robot's inspection. The calculation results reflect the degree of change in the accuracy of the algorithm in controlling the trajectory under different working conditions. In order to meet the control requirements of robot trajectory for inspection work, the $\Delta\hat{\theta}_\Sigma$ value of the steering angle of the tunnel inspection drone is required to be less than 1.9° during testing.

In order to verify the effect of robust control of the trajectory of the roadway inspection robot, the proposed method is utilized to control the inspection trajectory of the robot and observe the degree of coincidence with the ideal trajectory; the more consistent it is, the better the effect of robust control of the trajectory.

To further verify the robustness of the trajectory control, the robot's inspection position results under the control method are compared to the actual positions; the smaller the deviation, the better the control effect.

3.3 Analysis of results

Analysis of the effectiveness of PID control parameter tuning

The algorithm in the article optimizes the control parameters of the PID controller through a fuzzy neural network when controlling the trajectory of the tunnel inspection robot, and its optimisation effect directly affects the subsequent control. Therefore, the trajectory control of the tunnel inspection robot is carried out by optimizing the controllers before and after, respectively, to verify the optimisation effect of fuzzy neural network on the control parameters of PID controller. The steering angle control results before and after optimisation are shown in *Figure 6*.

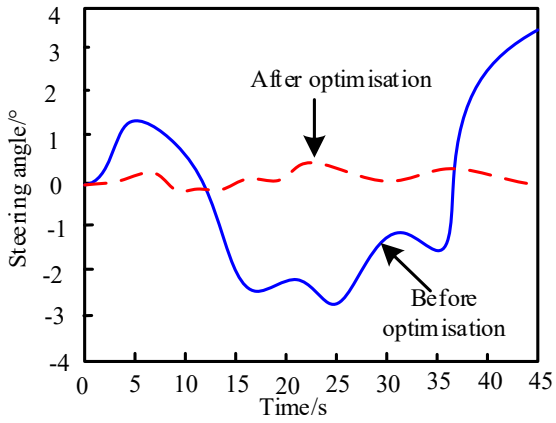

Figure 6 – Control result of steering angle

The analysis of the test results in *Figure 6* shows that before the optimisation of PID control parameters, the steering angle deviation of the roadway inspection robot is between ±4°. After the optimisation of PID control parameters for robot trajectory control, the steering angle deviation is between ±1°. Because the method in the paper uses a fuzzy neural network to optimise the PID control parameters, the robot's speed error and steering angle error are used as input variables, which output the adjustments to the PID parameters, thereby ensuring the controller's effectiveness.

Analysis of indicator results

After the trajectory control of the roadway inspection robot by the algorithm in the paper, under different inspection distances, in a single scenario (usually refers to the relatively simple, clear and repetitive inspection environment in the coal mine roadway. In this scenario, the inspection robot needs to accomplish relatively fixed tasks) and complex scenarios (the roadway may have complex terrain such as curved, narrow, cross, etc. and the robot needs to accomplish multiple tasks at the same time), after the control by the algorithm in the paper, the calculation results of the robustness margin index $\Delta\hat{\theta}_{\Sigma}$ are shown in *Table 3*.

Table 3 – Test results of robustness margin index (°)

Inspection distance /m	Inspection scene	
	Single scene	Complex scenes
15	0.65	0.95
30	0.80	1.30
45	0.55	1.55
60	0.40	1.40
75	0.80	1.67
90	1.50	1.85
105	0.50	1.2
120	0.96	1.56
135	1.25	1.70
150	1.03	1.69

Analysing the test results in *Table 3*, it can be seen that in a single scene and a complex scene, with the continuous change of the inspection distance of the roadway inspection robot, after the robot trajectory control by using the method in the paper, the calculation results of the steering angle robustness margin index $\Delta\hat{\theta}_{\Sigma}$ are lower than 1.9°. The steering angle robustness margin index $\Delta\hat{\theta}_{\Sigma}$ in a single scene is 1.5°, and the steering

angle robustness margin index $\Delta\hat{\theta}_{\Sigma}$ in a complex scenario is 1.85°. Therefore, the control algorithm proposed in the paper has good control robustness and meets the control standard of the robot.

To thoroughly verify the robustness of the trajectory control algorithm proposed in the paper for the alley inspection robot, an ideal trajectory is set. The robot's inspection trajectory control results under complex conditions are then obtained using the algorithm. The degree of coincidence between the controlled inspection trajectory and the ideal trajectory is evaluated, and the test results are shown in *Figure 7*.

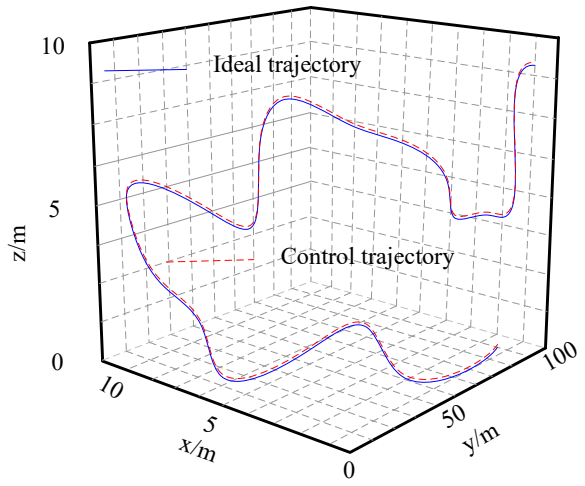

Figure 7 – Trajectory control results in complex inspection scenarios

Analysing the test results in *Figure 7*, it can be seen that after the inspection trajectory control of the roadway inspection robot by the algorithm in the paper, the control results in the complex inspection scenario have a high degree of agreement with the ideal results of the setup, and there is no significant trajectory bias, and even in the large curvature of the trajectory control results can still maintain a better match. Therefore, this method is able to accomplish the robust control of the trajectory of the roadway inspection robot.

To further verify the robust control effect of the algorithm in the article on the trajectory of the tunnel inspection robot, the algorithm was applied to the inspection of the robot in the mine tunnel. The inspection area is a high-temperature danger zone, and 10 key inspection trajectory positions were set during the inspection process (all located at corners, intersections, and slope areas). From this, the inspection results of the robot at 10 key positions under the control of the method described in the article were obtained, as shown in *Table 4*.

Table 4 – Inspection trajectory control results (cm)

Key position	Key point location	Trajectory control results
1	(2.3,42.5)	(2.5,42.5)
2	(2.5,30)	(2.5,30)
3	(4.2,20)	(4.2,20)
4	(7.6,20)	(7.5,20)
5	(10.6,18.6)	(10.5,18.6)
6	(10,40.3)	(10,40.3)
7	(12.2,30.6)	(12.2,30.5)
8	(11.7, 6.5)	(12, 6.5)
9	(17.7, 19.8)	(17.7, 20)
10	(17.7, 44.3)	(17.7, 44.3)

Analysing the test results in *Table 4*, it can be seen that during the inspection process, the alleyway robot, under the robust trajectory control of the proposed method, was able to accurately follow the ideal inspection trajectory. This ensures both the safety and comprehensiveness of the inspection process. After applying the control method, the robot's trajectory accuracy in the X and Y directions showed a maximum deviation of only (0.3, 0) cm. This demonstrates the method's ability to handle system uncertainty and ambiguity while remaining insensitive to small input variations. As a result, it offers strong robustness and can adapt to real-world conditions, allowing the robot to operate reliably in a variety of complex environments.

3.4 Comparative analysis of algorithm performance

On the basis of detailed verification of the performance of the trajectory robust control algorithm for tunnel inspection robots based on fuzzy neural networks proposed in this paper, a comprehensive comparison was conducted with several state-of-the-art trajectory control algorithms to better clarify its position and advantages within existing research. Specifically, compared with model-based predictive control (MPC), the algorithm proposed in this paper significantly reduces computational complexity and can adaptively adjust PID parameters through fuzzy neural networks, thereby reducing dependence on the system model and demonstrating higher real-time performance and robustness. However, when dealing with complex trajectory tracking problems that require long-term optimisation, MPC may have more refined control capabilities. Although adaptive control can adjust parameters online to adapt to dynamic changes in the system, its algorithm design and implementation are relatively complex, and the convergence speed and steady-state performance may be affected by multiple factors. In contrast, the algorithm proposed in this paper achieves faster and more intelligent parameter adjustment through fuzzy neural networks, especially when dealing with nonlinear and uncertain factors in tunnel environments. In addition, compared with PID control optimised by genetic algorithm, this algorithm does not require time-consuming optimisation calculations in advance, but achieves online real-time parameter adjustment, thus occupying advantages in real-time performance and flexibility. However, in static environments that require extremely high control accuracy, PID control that has been fully optimised may exhibit higher control accuracy. In summary, the trajectory robust control algorithm for tunnel inspection robots based on fuzzy neural networks proposed in this paper performs well in trajectory control accuracy, response speed and robustness, and is particularly suitable for complex and changing tunnel environments, although it may be slightly inferior to other algorithms in certain specific environments.

4. CONCLUSION

This paper proposes a fuzzy neural network-based robust control algorithm for the trajectory of the roadway inspection robot by combining the environmental specificity and motion characteristics of the roadway inspection robot in the inspection process. Combining the PID controller and fuzzy neural network, the PID control parameters are dynamically adjusted through the introduction of fuzzy neural network, so that the roadway inspection robot can not only cope with the complex dynamic environmental changes but also maintain the accuracy of inspection trajectory through automatic adjustment when there are problems in the network performance. This adaptive ability and fault tolerance make the algorithm work properly under high temperature, cooling and other extreme conditions, ensuring that the robot can maintain stable trajectory tracking in the face of various uncertainties and disturbances, thus improving inspection efficiency and safety. In the future, the structure and parameters of fuzzy neural networks will be further optimised to improve their learning and generalization abilities, in order to adapt to more complex and changing tunnel environments.

REFERENCES

[1] Usova AA, et al. Stabilization of robot-environment interaction through generalized scattering techniques. *IEEE Transactions on Robotics*. 2022;38(2):1319-1333. DOI: 10.1109/TRO.2021.3107231.

[2] Yamagami M, et al. Effect of handedness on learned controllers and sensorimotor noise during trajectory-tracking. *IEEE Transactions on Cybernetics*. 2023;53(4):2039-2050. DOI: 10.1109/TCYB.2021.3110187.

[3] Rajendran V, et al. Towards autonomous selective harvesting: A review of robot perception, robot design, motion planning and control. *Journal of Field Robotics*. 2024;41(7):2247-2279. DOI: 10.1002/rob.22230.

[4] Duan J, et al. Design method of intelligent ropeway type line changing robot based on lifting force control and synovial film controller. *Journal of Robotics*. 2022;2022(Pt.1):3640851.1- 3640851.11. DOI: 10.1155/2022/3640851.

[5] Hacene N, et al. Comparison between fuzzy and non-fuzzy ordinary if-then rule-based control for the trajectory tracking of a differential drive robot. *International Journal of Fuzzy Systems*. 2022;24(8):3666-3687. DOI: 10.1007/s40815-022-01365-1.

[6] Liu S, Wang F, Li BL. Simulation of robot trajectory tracking control under nonholonomic constraints. *Computer Simulation*. 2023;40(10):422-425+444. DOI: 10.3969/j.issn.1006-9348.2023.10.081.

Jafari-Tabrizi A, Gruber DP, Gams, A. Exploiting image quality measure for automatic trajectory generation in robot-aided visual quality inspection. *The International Journal of Advanced Manufacturing Technology*. 2024;132(9/10):4885-4901. DOI: 10.1007/s00170-024-13609-5.

[7] Morlock M, et al. End-effector trajectory tracking of flexible link parallel robots using servo constraints. *Multibody System Dynamics*. 2022;56(1):1-28. DOI: 10.1007/s11044-022-09836-x.

[8] El Baji O, Amrani NBS, Sarsri D. Online trajectory tracking control based on the explicit form of the equations of motion for serial manipulator using the new formulation. *Journal of Robotics*. 2022;2022(Pt.2): 8715161.1-8715161.14. DOI: 10.1155/2022/8715161.

[9] Salvioli F, et al. Globally-optimal whole body motion planning under nonholonomic constraints using dynamic programming. *Acta Astronautica*. 2022;193:619-626. DOI: 10.1016/j.actaastro.2021.12.013.

[10] Salimi-Bad, A, Ebadzadeh MM. A novel learning algorithm based on computing the rules' desired outputs of a TSK fuzzy neural network with non-separable fuzzy rules. *Neurocomputing*. 2022;470:139-153. DOI: 10.1016/j.neucom.2021.10.103.

[11] Seyfi NS, Khalaji AK. Robust Lyapunov-based motion control of a redundant upper limb cable-driven rehabilitation robot. *Robotica: International Journal of Information, Education and Research in Robotics and Artificial Intelligence*. 2022;40(10):3355-3377. DOI: 10.1017/S0263574722000261.

[12] Chen F, et al. ConservationBots: Autonomous aerial robot for fast robust wildlife tracking in complex terrains. *Journal of Field Robotics*. 2024;41(2):443-469. DOI: 10.1002/rob.22270.

[13] Bisht RS, Pathak PM, Panigrahi SK. Modelling, simulation and experimental validation of wheel and arm locomotion based wall-climbing robot. *Robotica: International Journal of Information, Education and Research in Robotics and Artificial Intelligence*. 2022;41(2):433-469. DOI: 10.1017/S026357472200025X.

[14] Nasiri H, Ebadzadeh MM. MFRFNN: Multi-functional recurrent fuzzy neural network for chaotic time series prediction. *Neurocomputing*. 2022;507:292-310. DOI: 10.1016/j.neucom.2022.08.032.

[15] Nguyen HB, et al. Fuzzy hybrid neural network control for uncertainty nonlinear systems based on enhancement search algorithm. *International Journal of Fuzzy Systems*. 2022;24(8):3384-3402. DOI: 10.1007/s40815-022-01374-0.

[16] Mohammadzadeh A, et al. Fourier-based type-2 fuzzy neural network: Simple and effective for high dimensional problems. *Neurocomputing*. 2023;547:126316.1-126316.12. DOI: 10.1016/j.neucom.2023.126316.

[17] Almaghout K, et al. RBF neural network-based admittance PD control for knee rehabilitation robot. *Robotica: International Journal of Information, Education and Research in Robotics and Artificial Intelligence*. 2022;40(12):4512-4534. DOI: 10.1017/S0263574722001084.

[18] Canbek KO, Yalcin H, Baran EA. Drift compensation of a holonomic mobile robot using recurrent neural networks. *Intelligent Service Robotics*. 2022;15(3):399-409. DOI: 10.1007/s11370-022-00430-w.

[19] Bingul Z, Karahan O. Real-time trajectory tracking control of Stewart platform using fractional order fuzzy PID controller optimized by particle swarm algorithm. *Industrial Robot*. 2022;49(4):708-725. DOI: 10.1108/IR-07-2021-0157.

[20] Padmanaban J, et al. Sustainability study and SWOT analysis of mixed biofuel blends in engine at various injection pressure analysed by experimentally and statistically. *Scientific Reports*.2024;14:31574. DOI: 10.1038/s41598-024-79073-z.

[21] Mésároš P, et al. Factors influencing defects in residential buildings. *Journal of Building Pathology and Rehabilitation*. 2024;9:31. DOI: 10.1007/s41024-023-00381-4.